



Original research article

Antibacterial and cytotoxicity effects of biogenic palladium nanoparticles synthesized using fruit extract of *Couroupita guianensis* Aubl.



Sathishkumar Gnanasekar^a, Jeyaraj Murugaraj^b, Balakrishnan Dhivyabharathi^a,
Varunkumar Krishnamoorthy^c, Pradeep K Jha^d, Prabukumar Seetharaman^a,
Ravikumar Vilwanathan^c, Sivaramakrishnan Sivaperumal^{a,*}

^a Bharathidasan University, School of Biotechnology and Genetic Engineering, Department of Biotechnology, Tiruchirappalli 620024, Tamil Nadu, India

^b University of Madras, National Centre for Nanosciences and Nanotechnology, Chennai 600025, Tamil Nadu, India

^c Bharathidasan University, School of Life Sciences, Department of Biochemistry, Tiruchirappalli 620024, Tamil Nadu, India

^d Indian Institute of Technology Kharagpur, School of Medical Science and Technology, Kharagpur 721302, West Bengal, India

ARTICLE INFO

Article history:

Received 25 November 2016

Received in revised form 20 May 2017

Accepted 10 October 2017

Available online 7 November 2017

Keywords:

Palladium nanoparticles

X-ray diffraction

Polyols

Bactericidal

Lung cancer

ABSTRACT

Herein, we report a facile route to synthesize palladium nanoparticles (CGPdNPs) using the aqueous fruit extract of *C. guianensis* Aubl. as a potent biological reducing agent. Reduction of PdCl₂ solution into their nano scale was confirmed with the formation of a black precipitate which gives a reduced absorbance in UV–vis spectroscopy. Fourier transform infrared spectroscopy (FTIR) reveals the active role of phenolic constituents from *C. guianensis* in reduction and surface functionalization of nanoparticles (NPs). Dynamic light scattering (DLS) and zeta potential analysis confirms the generation of polydispersed highly stable NPs with large negative zeta value (−17.7 mV). Interestingly, X-ray Diffraction (XRD) pattern shows that the synthesized CGPdNPs were face centered cubic crystalline in nature. The HRTEM micrographs of CGPdNPs displays well-dispersed, spherical NPs in the size ranges between 5 and 15 nm with an average of 6 nm. It was also noticed that the synthesized CGPdNPs possess an effective antimicrobial activity against different bacterial pathogens. On the other hand, *in vitro* cell viability (MTT) assays reveals that the synthesized CGPdNPs exhibited an extraordinary anticancer properties. Eventually, hemocompatibility assay depicts the safe nature of synthesized NPs for biomedical application.

© 2017 Faculty of Health and Social Sciences, University of South Bohemia in Ceske Budejovice. Published by Elsevier Sp. z o.o. All rights reserved.

Introduction

The development of green chemistry route to obtain nano scale values of noble metals with different chemical compositions, sizes, shapes and tunable properties have received considerable attention due to their unique applications in electronics, catalysis, environmental remediation, diagnosis, targeted drug/gene delivery and antimicrobials (Basavegowda et al., 2014). However, several physical and chemical methodologies such as radiation, ablation, thermal decomposition, electro and sonochemical methods existed for nanoparticles preparation. Most of these methods were associated

with the utilization of toxic chemicals, intensive energy, and capital consumption (Govindarajan et al., 2017). As a low-cost eco-friendly alternative different biological entities such as bacteria (Klaus et al., 1999), fungi (Mukherjee et al., 2001), actinomycetes (Ahmad et al., 2003), yeast (Kowshik et al., 2002), algae (Xie et al., 2007) and plants (Sathishkumar et al., 2012) have been established to produce nanoparticles of noble metals. In compared with the microbial route, plant extract mediated NPs synthesis was receiving many preferences because of its reliability and easy scaling-up procedures (Mittal et al., 2013).

Moreover, an outbreak of deadliest diseases like malaria, cholera, tuberculosis and prevalence of multi-drug resistance (MDR) were the most important global health issues (Fayaz et al., 2010). Likewise, cancer continues to be the most potent scourges of mankind that causes major mortality rate every year worldwide (Misra et al., 2010). Lung cancer was one of the most common fatal cancers that causes severe mortality worldwide. According to

* Author for correspondence: Bharathidasan University, School of Biotechnology and Genetic Engineering, Department of Biotechnology, Palkalaiperur, Tiruchirappalli, Tamil Nadu 620024, India.

E-mail address: sivaramakrishnan123@yahoo.com (S. Sivaperumal).

International Agency for Research on Cancer (IARC) of the World Health Organization (WHO), it was reported that around 1.8 million (13% of total) new lung cancer cases were diagnosed and about 1.6 million (19.4% of total) deaths occurred due to lung cancer (Ferlay et al., 2012).

In spite of chemotherapy, early diagnosis and existence of targeted drugs lung cancer still remains the leading cause of mortality. Current cancer chemotherapy suffers from certain limitations like poor drug distribution, solubility, insufficient drug concentrations, unbearable toxicity and inadequate ability to monitor therapeutic responses. This situation urges to design new strategies, tools, and drugs for the diagnosis and treatment of cancer (Torre et al., 2015).

Generally, nanomaterials of noble metals such as gold (Au), silver (Ag), copper (Cu), platinum (Pt), palladium (Pd), iron (Fe), zinc (Zn) and titanium (Ti) have gained colossal attention due to their indispensable physio-chemical properties relative to their macro scale counterparts (Parhi et al., 2012). Also, these nanomaterials have shown extraordinary pharmaceutical applications like drug delivery, imaging, cell labelling, Surface-Enhanced Raman Scattering (SERS) detection, antioxidant, anti-inflammatory, bactericidal and cancer theranostics (Kharissova et al., 2013). Especially, metal and metal oxide nanomaterials were known to possess high potential in cancer management based on the selective disruption of mitochondrial respiratory chain leading to the production of reactive oxygen species (ROS) which in turn cause DNA damage (Mata et al., 2015; Sathishkumar et al., 2015). Among them, palladium nanoparticles (PdNPs) were recognized as a unanimous catalyst in many industrial applications. However, there were only very few studies have emphasized the distinct features of PdNPs for their applications as a drug delivery system, photothermal agents and anti-cancer/anti-microbial therapy (Dumas and Couvreur, 2015).

C. guianensis Aubl., commonly known as ayahuma and cannonball tree, belongs to *Lecythidaceae* family and possesses many medicinal properties such as antibiotic, antifungal, anticancer, antiulcer, antiseptic, and analgesic qualities. Extracts from this tree were used to cure colds and stomach aches and juice made from the leaves were used to cure malaria (Al-Dhabi et al., 2012). Hence, in the present study high phenolic enriched *C. guianensis* aqueous fruit extract was employed for the green synthesis of CGPdNPs towards valuable biomedical applications.

Materials and methods

Materials

Palladium (II) chloride (PdCl_2) was purchased from Sigma-Aldrich Mumbai, India. Dulbecco's modified eagle medium (DMEM), fetal bovine serum (FBS), antibiotics, trypsin-EDTA, phosphate buffer saline, nutrient broth, agar-agar, streptomycin sulphate, sterile paper discs and other chemicals were purchased from Himedia Laboratories, India. Fresh and healthy cannonball fruits (*C. guianensis*) were collected from Gokarnesvarar temple, Pudukkottai town, Tamil Nadu State, India. A549 cell line was procured from National Centre for Cell Sciences (NCCS), Pune, India. Bacterial pathogens used in this study *S. aureus* MTCC 96, *R. rhodochrous* MTCC 265, *E. coli* MTCC 1687, *P. mirabilis* MTCC 425, *P. aeruginosa* MTCC 1688, *V. cholerae* MTCC 3906, *B. cereus* MTCC 1272, *S. typhi* MTCC 3917, *M. luteus* MTCC 1809, *K. pneumonia* MTCC 530 were obtained from Microbial type culture and collection (MTCC), Chandigarh, India.

Preparation of fruit extracts (CGFE)

The collected fruit samples were cut into small pieces after removing their peel then washed thrice with distilled water to

remove other impurities and allowed to dry in shade condition for 5–10 days. After that, the well dried fruit samples were finely grounded using stainless steel kitchen blender to obtain fine powder. Subsequently, extract for the synthesis of CGPdNPs was prepared by simple decoction method, for that 10 g of sterilized fruit powder was mixed with 200 ml of Milli-Q water and kept in boiling water bath (60°C) for 20 min. Finally, the 5% extract was filtered through Whatmann no.1 filter paper and stored at 4°C for further studies.

Synthesis of CGPdNPs

To synthesize CGPdNPs, the reaction mixture was prepared by blending 5 ml (5%) of CGFE in 95 ml of 1 mmol/l substrate (PdCl_2 : 0.017 in 100 ml) and kept at room temperature under continuous stirring (Vimala et al., 2015). After that, the reaction mixture was checked for intense blackish colour formation and the absorbance maxima were monitored using UV–vis spectroscopy. Finally, the synthesized CGPdNPs was purified by repeated centrifugation at 16,000 rpm for 10 min at 4°C and the unreacted ions and molecules colloidal in CGPdNPs suspension was then dialyzed repeatedly by using a cellulose tube (MWcutoff 12400D) against 1000 ml of deionized water for 9 h at 30°C . Finally, the purified CGPdNPs were resuspended in Milli-Q water and then used for further characterization.

UV–visible spectroscopy

Initially, the reduction of Pd II ions was monitored based on the absorbance spectra in UV–vis Spectroscopy. For that, an aliquot of colloidal CGPdNPs was diluted with deionized water and the absorbance maxima were scanned in UV–vis spectrophotometer (Perkin-Elmer Lambda 2 UV198) at the wavelength of 300–700 nm.

FTIR and XRD analysis

FTIR analysis was achieved to determine the possible bio-compounds present in CGFE responsible for reduction and stabilization of CGPdNPs. Transmittance were measured for extract before and after addition of PdCl_2 , to perform FTIR the samples were grounded well with KBr powder and pelletized, afterwards the spectra were recorded in JASCO 460 PLUS FTIR spectrometer at the wavelength of 4000 cm^{-1} – 400 cm^{-1} . Further, the X-ray diffraction (XRD) study was performed at 40 kV and 30 mA using X-ray diffractometer (Ultima-III, Rigaku, Japan, $\lambda = 1.54\text{ \AA}$) with Cu Ka radiation ($k = 1.5406\text{ \AA}$) in the range of 20 – 80° at a scan speed of 2/min.

DLS, HRTEM, EDAX and SAED measurements

Hydrodynamic size distribution and surface charge of synthesized CGPdNPs were measured using dynamic light scattering (DLS) and zeta potential. To execute DLS, the colloidal CGPdNPs solution was further diluted and kept in water bath sonicator for 10–20 min to disperse the particles, size distribution measurements and zeta values were recorded using Malvern Zetasizer, Nano –ZS90 analyzer. The size and shape of synthesized CGPdNPs were measured with the micrographs obtained from JEOL JEM 2100 high resolution transmission electron microscope. For HRTEM analysis, the colloidal purified Pd solution allowed for sonication, a drop of this solution was used to make a thin film onto copper coated grid, allowed for drying under infrared lamp and micro graphical images of CGPdNPs were taken at different magnifications. Additionally, the presence of elemental palladium (Pd) in the mixture and their crystallinity were identified using an EDAX and SAED analysis.

Antimicrobial activity (Disc diffusion method)

Synthesized CGPdNPs was tested for its potential antimicrobial activity against bacterial human pathogens. To study antimicrobial

activity, the synthesized CGPdNPs and CGFE were subjected to disc diffusion method (Sathishkumar et al., 2012). The bacterial cultures were swabbed on individual nutrient agar medium, then the crude CGFE, synthesized CGPdNPs, positive control (streptomycin sulphate 1 mg/ml) and a negative control (distilled water) were loaded in sterile discs (6 mm) at the concentration 25 µg/ml. After drying, discs were impregnated onto the surface of inoculated medium and kept at 37 °C for 24 h, the different levels of zone of inhibition were measured using meter ruler.

In vitro anticancer activity

Cell lines and culture medium

Lung cancer cell line (A549) was cultured in DMEM supplemented with 10% inactivated Fetal Bovine Serum (FBS), penicillin (100 IU/ml), streptomycin (100 µg/ml) and amphotericin B (5 µg/ml) in humidified atmosphere of 5% CO₂ at 37 °C until confluent. The cells were dissociated with trypsin solution (0.2% trypsin, 0.02% EDTA, 0.05% glucose in PBS) and the stock cultures were grown in 25 cm² culture flasks.

Cell viability

The cytotoxic activity of CGFE and CGPdNPs were measured using the MTT (3-(4, 5-dimethylthiazol-2-yl)-2, 5-diphenyl tetrazolium bromide) assay (Mosmann, 1983). Briefly, the cells were seeded in 96-well plate at a density of 1×10^4 cells/well and allowed to grow for 24 h at 37 °C in the presence of 5% CO₂. After 24 h, the cells with 70–80% confluency were treated with 100 µg fresh incomplete DMEM medium containing different concentrations of the CGFE and CGPdNPs (1, 5, 10, 25, 50, 75, 100, 150, 200 and 250 µg/ml⁻¹) and incubated for 24 h. At the end of incubation, fresh media containing 0.40 mg/ml MTT was added to the 96-well plate and incubated for another 4 h at 37 °C in 5% CO₂. The formazan crystals developed after 4 h were solubilized with 100 µl of DMSO after aspirating the medium. Subsequently, the absorbance was monitored at 595 nm using a plate reader (Bio-Rad, Hercules, CA, USA). Growth inhibition was determined using:

$$\text{Growth inhibition} = (\text{control O.D.} - \text{sample O.D.}) / \text{control O.D.}$$

The results were expressed as mean values (\pm SD) of six repeats and IC₅₀ value was determined as the concentration of NPs that gives 50% reduction of cell viability.

Hemocompatibility assay

To assess the biocompatibility of synthesized CGPdNPs a hemolytic assay was performed as per our earlier report (Sathishkumar et al., 2016) with slight modification. For that, the fresh blood samples were collected from healthy volunteers in sterile lithium heparin vacutainers and then the red blood cells (RBCs) were separated by centrifugation at 1500 rpm for 10 min, followed by ficoll density gradient and finally the RBCs were further diluted in 20 mmol/l HEPES buffered saline (pH 7.4) to 5% v/v solution. Then, the samples CGFE and CGPdNPs were suspended in 10 mmol/l HEPES buffer saline. The RBC suspension was added to HEPES saline (NC), 1% Triton X-100 (PC) and samples at different concentration of (25, 50, 75 and 100 µg/ml) and incubated at 37 °C for 30 and 60 min. All samples were prepared in triplicate and after being slightly vortexed the suspension was incubated at static conditions for 4 h at 37 °C. After incubation, all the samples were centrifuged at 12,000 rpm at 4 °C and supernatants were transferred to a 96-well plate. The hemolytic activity was determined by measuring the absorbance at 570 nm (Biorad microplate reader model 550, Japan). Control samples of 0% lysis (in HEPES buffer)

and 100% lysis (in 1% Triton X-100) were employed in the experiment. The percent of hemolysis was calculated as follows:

$$\text{Hemolysis\%} = [(\text{sample absorbance} - \text{negative control}) / (\text{positive control} - \text{negative control})] \times 100$$

This study was approved by the Institutional ethics committee (IEC) of Bharathidasan University (Ref No. DM/2014/101/54).

Results and discussion

Plant-mediated green chemistry approach to fabricate nano-structures of noble metals have drawn huge attention as facile, cost-effective and commercially viable alternative to conventional chemical and physical methods (Narayanan and Sakthivel, 2011). Also, utilization of natural extracts as a reducing and stabilizing agent for nanoparticles preparation will deliver biocompatible end-products. Here, we have examined the ability of *C. guianensis* phytochemicals to interact with Pd (II) ions and reduce them into nano scale values.

Synthesis of CGPdNPs

Synthesis started with the reduction of Pd (II) ions into Pd⁰ and complexes with active phenolic constituents and reducing sugars of CGFE, which turns the colour of reaction mixture from brown to greenish black after 24 h of continuous stirring at room temperature (Fig. 1a). Our result highly corroborating with an earlier report (Kanchana et al., 2010) where, PdNPs synthesized using the *S. trilobatum* gives black colour precipitation mainly due to collective oscillation of electrons. Nevertheless, the exact mechanism of biosynthesis was still not clear. Presumably, the hydroxyl group containing polyols plays a crucial role in the reduction process (He et al., 2009). It was well demonstrated earlier that the gallic acid present in *D. regia* leaf extract donates an electron and easily oxidize into its quinones form, PdCl₂ first oxidize gallic acid and forms an intermediate palladium complex (Dauthal and Mukhopadhyay, 2013). The Pd²⁺ ion then reduced to Pd⁰ in the presence of free electron or nascent hydrogen, which were produced during bioreduction reaction. Finally, collision of the neighbouring Pd⁰ atoms leads to the formation of PdNPs. Based on the above fact, our results represent that the active phenolic constituents of CGFE were mainly responsible for PdNPs reduction and surface functionalization.

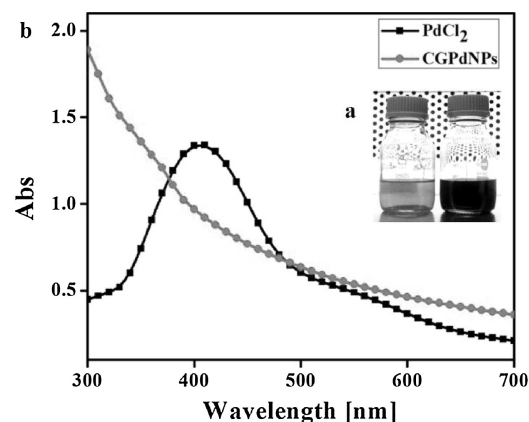


Fig. 1. Synthesis of CGPdNPs. (a) Aqueous PdCl₂ was exhibiting light brown colour, whereas formation black precipitate confirms the synthesis of CGPdNPs from CGFE; (b) UV-visible spectroscopy shows the reduced absorbance spectra for synthesized CGPdNPs.

Characterization of CGPdNPs

The UV–vis absorbance spectra showed the maximum absorbance at 420 nm for the reference sample PdCl_2 due to existence of Pd (II) ions. For CGPdNPs, the peak at 420 nm was entirely removed and a broad continuous absorption was observed, indicating the complete reduction of Pd (II) ions into CGPdNPs (Fig. 1b). The efficiency of CGFE in reduction of PdCl_2 was revealed by the reduced absorption, which was similar to the results of previous studies (Kumar et al., 2013; Shanthi et al., 2015). Additionally, FTIR analysis reveals the functional groups of absorbed biomolecules on the surface of nanoparticles. The transmittance for CGFE were observed at 3421.1 cm^{-1} , 2924.52 cm^{-1} , 1631.48 cm^{-1} , 1549.52 cm^{-1} , 1455.03 cm^{-1} , 1383.68 cm^{-1} , 1238.08 cm^{-1} , 1155.15 cm^{-1} , 1044.26 cm^{-1} , 705.819 cm^{-1} , 863.953 cm^{-1} , 601.68 cm^{-1} (Fig. 2). Vibrational stretches at 3421.1 cm^{-1} and 2924.52 cm^{-1} corresponds to O–H of phenol group and C–H stretching of aromatic compounds. The peak at 1631.48 cm^{-1} attributes C–C stretch in aromatic ring and it confirms the presence of aromatic group, whereas the transmittance peak at 1455.03 cm^{-1} manifests the O–H bend of polyphenol and weaker band at 1238.08 cm^{-1} assigned to C–O–C stretch. All vibrations confirmed that the identified functional groups in bio-organic moieties mainly polyols getting complexed with CGPdNPs in the aqueous medium (Sheny et al., 2012). Shift in the transmittance for generated CGPdNPs were mainly due to the interaction of phenolic constituents with nanomaterials during reduction and stabilization process (Guidelli et al., 2011). This also clearly implies that the binding of metal ions with hydroxyl and carboxylate groups of bio entities were used as reducing agent (Shen et al., 2009). The mechanism of bio-reduction of Pd (II) ions to PdNPs occurs upon binding of metal ions with the functional groups like hydroxyl (O–H) group of phenolic compounds, terpenoids, tanins, saponins, and reducing sugars, free amine groups of (N–H) amino acids and proteins (Kumari et al., 2015). Based on our earlier report (Sathishkumar et al., 2016), the fruit extract of CGFE possess large number active phenolic constituents which plays a crucial role in the coordination of (O–H) functional group with metal ions and converts Pd^{2+} into Pd^0 -flavanoid complex.

The crystalline structure and size of CGPdNPs were determined by XRD pattern, three distinct diffraction peaks at 40, 46.7 and 68 were indexed to reflections from (1 1 1), (2 0 0) and (2 2 0) planes (Fig. 3) that highly matches with the standard JCPDS card No. 87–0643, which denotes the face centered cubic (fcc-lattice) crystalline structure of PdNPs. Our data were significantly consistent with previous studies using different bioreductants such as coffee and

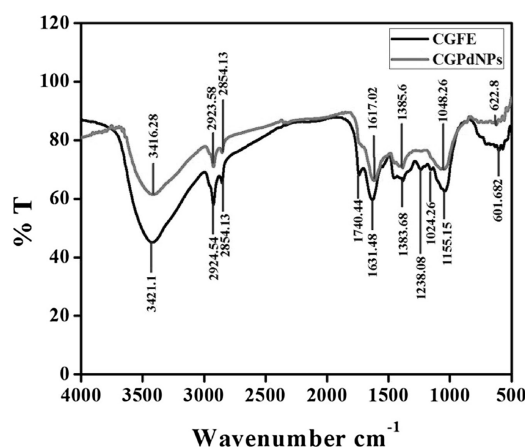


Fig. 2. FTIR analysis attributes the involvement of (O–H) group containing polyols from CGFE in reduction and stabilization of CGPdNPs.

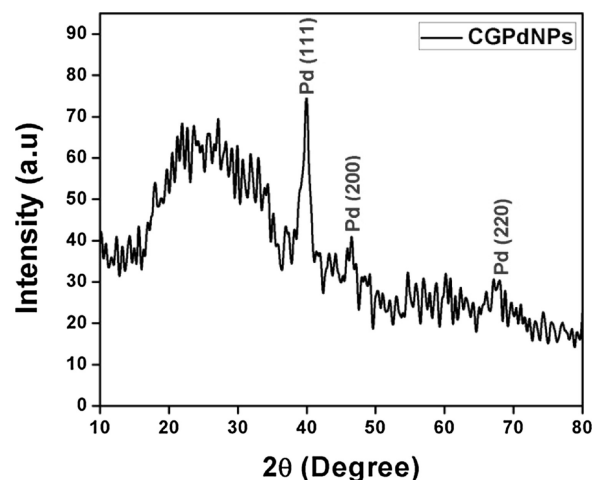


Fig. 3. XRD pattern of synthesized CGPdNPs displays the diffraction planes corresponds to the face centered cubic (fcc) structure.

tea extracts (Nadagouda and Varma, 2008) as well as the dried leaves of *A. occidentale* (Sheny et al., 2012) and *P. glutinosa* extract (Khan et al., 2014). The diffraction pattern and calculated lattice constants $a = 3.9115\text{ Å}$ and $v = 59.847\text{ Å}$ were in good agreement with standard diffraction data (JCPDS No. 87–0643). Also the mean crystalline size of CGPdNPs was calculated using Debye-Scherrer equation by determining the width of (1 1 1) peak and was found to be 5.06 nm respectively which was in fair agreement with the HRTEM measurements.

DLS size distribution intensity confirms the stability and dispersity of synthesized CGPdNPs in the colloidal state. The hydrodynamic diameter of CGPdNPs was obtained as 27 nm (Fig. 4a). Similar results have been reported by Dauthal and Mukhopadhyay (2013) as compared to XRD and TEM analysis variation in the size of PdNPs, where it was mainly due to the presence of plant biomolecules. In addition, the stability of CGPdNPs solution was analyzed through zeta potential, which measures the surface electrostatic potential and mobility of

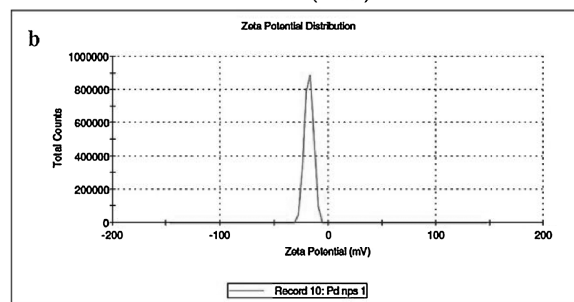
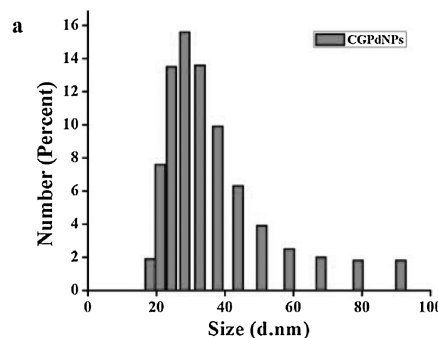


Fig. 4. (a) DLS analysis of CGPdNPs; and (b) Zeta potential measurement of CGPdNPs.

nanoparticles in colloidal suspension. Fig. 4b shows the zeta potential of CGPdNPs measured as -17.7 (mV) indicating that the largest negative potential value could be due to capping agent, which generates repulsive forces between the NPs in growth medium (Edison and Sethuraman, 2012).

To determine the morphology, size, and crystallinity HRTEM analysis was performed. It was interesting to note that almost all the particles were not in physical contact, the micrograph displays spherical, relatively good monodispersed and equally distributed CGPdNPs in the size range between 5 and 15 nm with an average diameter of 6 nm (Fig. 5a). The CGPdNPs size distribution was much smaller and narrow when compared to PdNPs synthesized using *T. chebula* aqueous extract (Kumar et al., 2013). In another study, a very similar particle HRTEM micrograph was reported, where PdNPs synthesized using *H. rhamnoides* L. leaf broth, the particles were found to be smaller and the inter particle distance was uniformly separated and well aligned size of 5 ± 2.5 nm (Nasrollahzadeh et al., 2015). The synthesized CGPdNPs were not involved in direct contact and no fusion between particles was noticed mainly due to the presence of biomolecules as capping agent (Ghaffari-Moghaddam and Hadi-Dabanlou, 2014).

Interestingly, a thin layer of biomolecular coating was clearly visualized, which seems to be the responsible compound in stabilization of nanoparticles (Ghaffari-Moghaddam et al., 2014). The SAED pattern suggests that the particles were highly crystalline nature as shown in Fig. 5b. It was apparent that the diffraction rings from inner to outer indicating the fcc phases of Pd with (1 1 1), (2 0 0) and (2 2 0) reflections, respectively. A similar phenomenon was observed for the PdNPs synthesized using leaves broth of Soybean (*G. max*) (Petla et al., 2012). Additionally, EDAX analysis shows a strong elemental peak signal for Pd of the highest

percentage, confirming the purity of CGPdNPs (Fig. 5c). Fig. 5d was the particle size distribution histogram of around 50 nanoparticles, which also authenticates that the synthesized CGPdNPs were polydispersed in nature.

Antibacterial activity

The antibacterial effect of aqueous CGFE and synthesized CGPdNPs were studied against bacterial human pathogens namely *S. aureus* MTCC 96, *R. rhodochorous* MTCC 265, *E. coli* MTCC 1687, *P. mirabilis* MTCC 425, *P. aeruginosa* MTCC 1688, *V. cholerae* MTCC 3906, *B. cerues* MTCC 1272, *S. typhi* MTCC 3917, *M. luteus* MTCC 1809, *K. pneumonia* MTCC 530. This was the first study to report antibacterial potential of biogenic CGPdNPs against 10 clinically isolated human pathogens. A clear zone of inhibition (ZOI) was noticed around each disc and the diameter in millimetre were determined (Fig. 6a). All the tested pathogens exhibit more susceptibility to CGPdNPs than CGFE denotes its enhanced antibacterial efficacy, no ZOI was observed for negative control.

CGPdNPs exhibits high level of bactericidal effect against *K. pneumonia* MTCC 530, *E. coli* MTCC 1687, *S. typhi* MTCC 3917 and *V. cholerae* MTCC 3906 moderate ZOI was seen for *S. aureus* MTCC 96, *R. rhodochorous* MTCC 265, *P. mirabilis* MTCC 425, *P. aeruginosa* MTCC 1688, *B. cerues* MTCC 1272 and *M. luteus* MTCC 1809 (Fig. 6b). Recently, it was reported that the bacterial inhibitory action of PdNPs mostly relies on the size, shape and composition (Adams et al., 2014). However, there was no clear mechanism of action it was believed that Pd^{2+} effectively inhibits creatine kinase, succinate dehydrogenase, and many other enzymatic processes in cells (Mallikarjuna et al., 2013). The exact mechanism of nano metals triggered antibacterial action were still being investigated, basically two phenomena has been proposed, firstly the toxicity arising due to the dissolution of metals from surface of nanoparticles and also oxidative stress via the generation of reactive oxygen species (ROS) on surfaces of nanoparticles (Ramalingam et al., 2016).

In vitro anticancer activity

An extensive MTT assay on A549 lung cancer cells was carried out to assess anticancer efficacy of synthesized CGPdNPs in different doses. As of now very few researchers have explored the anticancer potential of PdNPs, we found that the synthesized CGPdNPs effectively inhibit A549 cell viability than CGFE depicts the improved anticancer efficacy. Our results revealed that the biofunctionalized CGPdNPs shows high-level anticancer activity than crude CGFE in dose-dependent manner at 24 h time.

The IC₅₀ values of CGFE and CGPdNPs were determined to be 160 and $121 \mu\text{g/ml}^{-1}$ for 24 h treatment period respectively (Fig. 7). It was now well established that the apoptosis was the key event in cancer therapy which can be measured with the activation caspase-cascade, chromatin aggregation, partition of the cytoplasm and nucleus into membrane-bound vesicles (apoptotic bodies) that contain ribosomes, morphologically intact mitochondria, and nuclear material (Jeyaraj et al., 2015). Gurunathan et al. (2015) reported that the phyto-fabricated PdNPs shows dose-dependent cytotoxicity against treated human ovarian cancer cells. Detailed *in vitro* studies have proved that the PdNPs triggers cellular toxicity via generation of reactive oxygen species (ROS) which results in autophagy and eventually leads to autophagic cell death. Also, it was noticed that *E. alsinoides* PdNPs enhances caspase-3 activity that causes mitochondrial dysfunction and apoptosis. In another report, the PdNPs prepared from *S. aromaticum* activates cytochrome c and caspase 3, down regulates Bcl-2 and Bcl-XL that induces apoptosis mediated HeLa cell death (Shanthi et al., 2015). In this study CGPdNPs treated

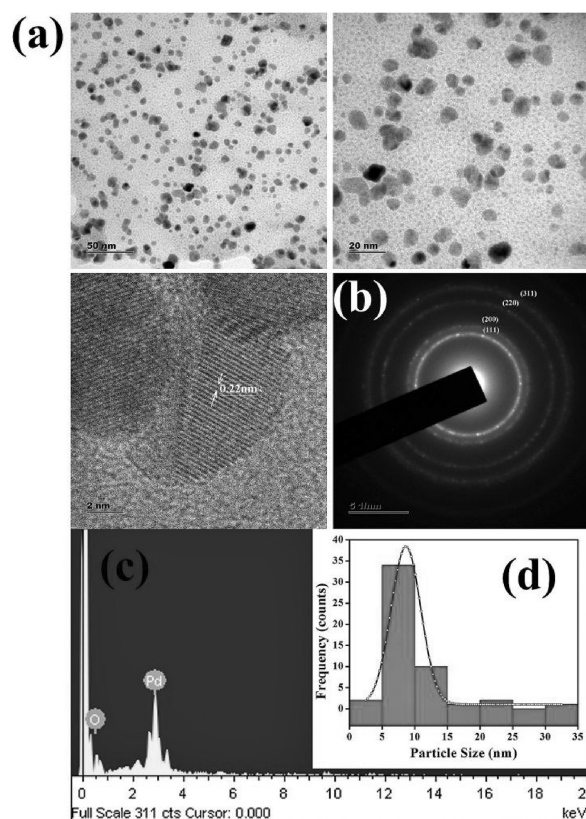


Fig. 5. (a) HRTEM micrograph of CGPdNPs displays well dispersed particles with the size range of 5–15 nm; (b) SEAD pattern of CGPdNPs; (c) EDAX analysis of CGPdNPs gives a strong signal for Pd; and (d) Particle size distribution histogram of synthesized CGPdNPs.

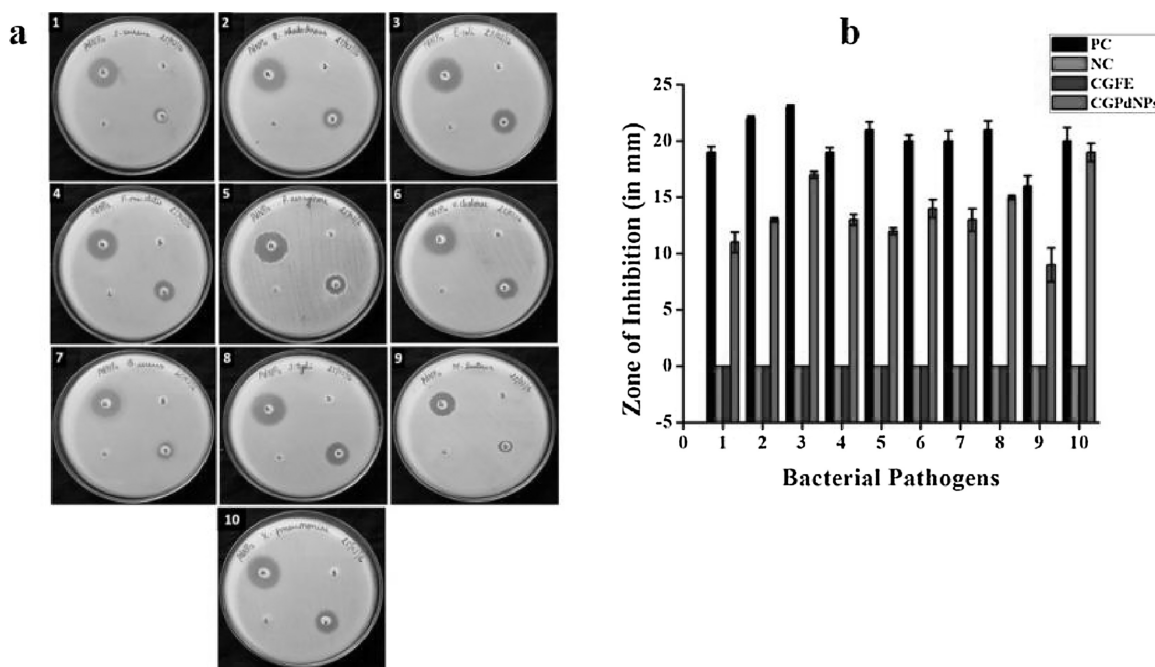


Fig. 6. (a) Antibacterial activity synthesized CGPdNPs against bacterial pathogens such as 1 – *S. aureus* MTCC 96, 2 – *R. rhodochlorus* MTCC 265, 3 – *E. coli* MTCC 1687, 4 – *P. mirabilis* MTCC 425, 5 – *P. aeruginosa* MTCC 1688, 6 – *V. cholerae* MTCC 3906, 7 – *B. cereus* MTCC 1272, 8 – *S. typhi* MTCC 3917, 9 – *M. luteus* MTCC 1809, 10 – *K. pneumoniae* MTCC 530; (b) Zone of inhibition of synthesized CGPdNPs against tested bacterial pathogens.

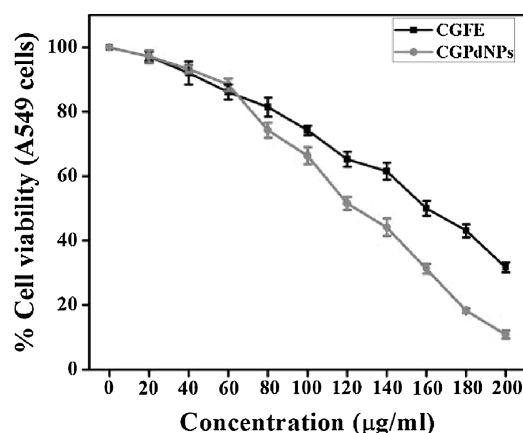


Fig. 7. *In vitro* anticancer activity of synthesized CGPdNPs: MTT assay results confirming the dose-dependent cytotoxicity efficacy of CGPdNPs against A549 cells after 24 h treatment. All the data expressed as the mean \pm SD of the three experiments with duplicate wells.

A549 cells lose their viability in dose dependent manner. Compareto plant extract ($160 \mu\text{g/ml}^{-1}$) synthesized CGPdNPs ($121 \mu\text{g/ml}^{-1}$) has shown increased cytotoxicity mainly due to increased synergetic effect, high-solubility, bioavailability and improved surface properties (Kajani et al., 2016).

Hemocompatibility assay

To assess the biocompatibility of synthesized CGPdNPs hemolytic assay was performed upon calculating the damage to human RBCs. The results showed that at $100 \mu\text{g/ml}$ concentration CGPdNPs (2.7%) exhibits comparatively very less acceptable level of red hemoglobin release than CGFE (4.2%) and positive control Triton-1X (100%), implying its safe nature in application (Fig. 8a and b). Our results demonstrated that the active biocompounds

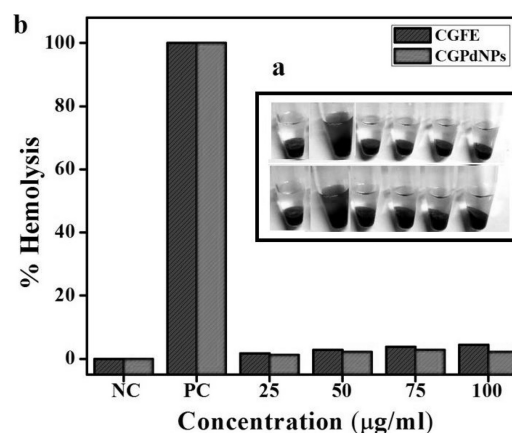


Fig. 8. (a) *In vitro* hemocompatibility assay of CGPdNPs demonstrates much less haemolytic activity than crude CGFE; (b) No (0%) lysis negative control (NC-HEPES buffer) whereas the positive control (PC – 1% Triton X-100) shows 100% lysis.

capped onto the surface of CGPdNPs largely strengthening its biocompatibility. Few earlier studies have proved that the surface passivation of nanoparticles with active biomolecules will improve their biocompatibility (Edison and Sethuraman, 2012). As reported earlier, the hemolytic permissible level for bio-based materials was less than 5% (Sathishkumar et al., 2015). Synthesized CGPdNPs were exhibits very less hemolytic activity which clearly denotes their biocompatibility and suitability for further clinical level demonstrations.

Conclusion

We report a facile, green chemistry route to synthesize PdNPs using the aqueous CGFE with easy scaling-up process. Extensive analytical techniques have revealed that the phenolic and phenolic acids enriched CGFE potentially generates well dispersed, highly stable, and crystalline PdNPs with stupendous surface properties.

The synthesized CGPdNPs have shown remarkable antibacterial activity against both gram positive and gram negative bacterial pathogens at 25 µg/ml dosage. Moreover, the anticancer prospective of the CGPdNPs in human lung carcinoma cells was notable with 50% of mortality at 121 µg/ml and the blood compatibility of synthesized CGPdNPs depicts that it does not interact with whole RBCs. The overall study implicates that the green synthesized CGPdNPs can be used as multifunctional hybrid nanomaterial for a wide spectrum of applications in nanomedicine such as imaging, drug delivery and therapeutics. Further, it was very important to study the signalling pathways involved with cellular toxicity, also the preclinical insights of formulated nanomaterials and these studies were in progress.

Conflict of interests

The authors declares no conflict of interests.

References

- Adams, C.P., Walker, K.A., Obare, S.O., Docherty, K.M., 2014. Size-dependent antimicrobial effects of novel palladium nanoparticles. *PLoS One* 9, 1–9.
- Ahmad, A., Senapati, S., Khan, M.I., Kumar, R., Sastry, M., 2003. Extracellular biosynthesis of monodisperse gold nanoparticles by a novel extremophilic actinomycete *Thermomonospora* sp. *Langmuir* 19, 3550–3553.
- Al-Dhabi, N.A., Balachandran, C., Raj, M.K., Duraipandian, V., Muthukumar, C., Ignacimuthu, S., et al., 2012. Antimicrobial: antimycobacterial and antibiofilm properties of *Couroupita guianensis* Aubl. fruit extract. *BMC Complement. Altern. Med.* 12, 1–8.
- Basavegowda, N., Idhayadhulla, A., Lee, Y.R., 2014. Preparation of Au and Ag nanoparticles using *Artemisia annua* and their *in vitro* antibacterial and tyrosinase inhibitory activities. *Mater. Sci. Eng. C* 43, 58–64.
- Dauthal, P., Mukhopadhyay, M., 2013. Biosynthesis of palladium nanoparticles using *Delonix regia* leaf extract and its catalytic activity for nitro-aromatics hydrogenation. *Ind. Eng. Chem. Res.* 52, 18131–18139.
- Dumas, A., Couvreur, P., 2015. Palladium: a future key player in the nanomedical field? *Chem. Sci.* 6, 2153–2157.
- Edison, T.J.I., Sethuraman, M.G., 2012. Instant green synthesis of silver nanoparticles using *Terminalia chebula* fruit extract and evaluation of their catalytic activity on reduction of methylene blue. *Process Biochem.* 47, 1351–1357.
- Fayaz, A.M., Balaji, K., Girilal, M., Yadav, R., Kalaichelvan, P.T., Venketesan, R., 2010. Biogenic synthesis of silver nanoparticles and their synergistic effect with antibiotics: a study against gram-positive and gram-negative bacteria. *Nanomedicine: Nanotechnology, Biol. Med.* 6, 103–109.
- Ferlay, J., Soerjomataram, I., Ervik, M., Dikshit, R., Eser, S., Mathers, C. et al., 2012. Cancer incidence and mortality worldwide: IARC CancerBase No. 11. *Globocan; 2012*. [online] [cit. 2013–15-04]. Available from: <http://globocan.iarc.fr>.
- Ghaffari-Moghaddam, M., Hadi-Dabanlou, R., 2014. Plant mediated green synthesis and antibacterial activity of silver nanoparticles using *Crataegus douglasii* fruit extract. *J. Ind. Eng. Chem.* 20, 739–744.
- Ghaffari-Moghaddam, M., Hadi-Dabanlou, R., Khajeh, M., Rakhshanipour, M., Shameli, K., 2014. Green synthesis of silver nanoparticles using plant extracts. *Korean J. Chem. Eng.* 31, 548–557.
- Govindarajan, M., AlQahtani, F.S., AlShebly, M.M., Benelli, G., 2017. One-pot and eco-friendly synthesis of silver nanocrystals using *Adiantum radicans*: Toxicity against mosquito vectors of medical and veterinary importance. *J. Appl. Biomed.* 15, 87–95.
- Guidelli, E.J., Ramos, A.P., Zaniquelli, M.E.D., Baffa, O., 2011. Green synthesis of colloidal silver nanoparticles using natural rubber latex extracted from *Hevea brasiliensis*. *Spectrochim. Acta, Part A* 82, 140–145.
- Gurunathan, S., Kim, E., Han, J.W., Park, J.H., Kim, J.H., 2015. Green chemistry approach for synthesis of effective anticancer Palladium nanoparticles. *Molecules* 20, 22476–22498.
- He, F., Liu, J., Roberts, C.B., Zhao, D., 2009. One-step green synthesis of Pd nanoparticles of controlled size and their catalytic activity for trichloroethene hydrodechlorination. *Ind. Eng. Chem. Res.* 48, 6550–6557.
- Jeyaraj, M., Renganathan, A., Sathishkumar, G., Ganapathi, A., Premkumar, K., 2015. Biogenic metal nanoformulations induce Bax/Bcl2 and caspase mediated mitochondrial dysfunction in human breast cancer cells (MCF 7). *RSC Adv.* 5, 2159–2166.
- Kajani, A.A., Zarkesh-Esfahani, S.H., Bordbar, A.K., Khosropour, A.R., Razmjou, A., Kardi, M., 2016. Anticancer effects of silver nanoparticles encapsulated by *Taxus baccata* extracts. *J. Mol. Liq.* 223, 549–556.
- Kanchana, A., Devarajan, S., Ayyappan, S.R., 2010. Green synthesis and characterization of palladium nanoparticles and its conjugates from *Solanum trilobatum* leaf extract. *Nano-Micro Lett.* 2, 169–176.
- Khan, M., Khan, M., Kuniyil, M., Adil, S.F., Al-Warhan, A., Alkhathlan, H.Z., et al., 2014. Biogenic synthesis of palladium nanoparticles using *Pulicaria glutinosa* extract and their catalytic activity towards the Suzuki coupling reaction. *Dalton Trans.* 43, 9026–9031.
- Kharissova, O.V., Dias, H.R., Kharisov, B.I., Pérez, B.O., Pérez, V.M.J., 2013. The greener synthesis of nanoparticles. *Trends Biotechnol.* 31, 240–248.
- Klaus, T., Joerger, R., Olsson, E., Granqvist, C.G., 1999. Silver-based crystalline nanoparticles, microbially fabricated. *Proc. Natl. Acad. Sci.* 96, 13611–13614.
- Kowshik, M., Ashtaputre, S., Kharrazi, S., Vogel, W., Urban, J., Kulkarni, S.K., Paknikar, K.M., 2002. Extracellular synthesis of silver nanoparticles by a silver-tolerant yeast strain MKY3. *Nanotechnology* 14, 95.
- Kumar, K.M., Mandal, B.K., Kumar, K.S., Reddy, P.S., Sreedhar, B., 2013. Biobased green method to synthesise palladium and iron nanoparticles using *Terminalia chebula* aqueous extract. *Spectrochim. Acta, Part A* 102, 128–133.
- Kumari, A.S., Venkatesham, M., Ayodhya, D., Veerabhadram, G., 2015. Green synthesis, characterization and catalytic activity of palladium nanoparticles by xanthan gum. *Appl. Nanosci.* 5, 315–320.
- Mallikarjuna, K., Sushma, N.J., Reddy, B.S., Narasimha, G., Raju, B.D.P., 2013. Palladium nanoparticles: single-step plant-mediated green chemical procedure using Piper beetle leaves broth and their anti-fungal studies. *Int. J. Chem. Anal. Sci.* 4, 14–18.
- Mata, R., Nakkala, J.R., Sadras, S.R., 2015. Biogenic silver nanoparticles from *Abutilon indicum*: their antioxidant, antibacterial and cytotoxic effects *in vitro*. *Colloids Surf. B: Biointerfaces* 128, 276–286.
- Misra, R., Acharya, S., Sahoo, S.K., 2010. Cancer nanotechnology: application of nanotechnology in cancer therapy. *Drug Discovery Today* 15, 842–850.
- Mittal, A.K., Chisti, Y., Banerjee, U.C., 2013. Synthesis of metallic nanoparticles using plant extracts. *Biotechnol. Adv.* 31, 346–356.
- Mosmann, T., 1983. Rapid colorimetric assay for cellular growth and survival: application to proliferation and cytotoxicity assays. *J. Immunol. Methods* 65, 55–63.
- Mukherjee, P., Ahmad, A., Mandal, D., Senapati, S., Sainkar, S.R., Khan, M.I., et al., 2001. Bioreduction of AuCl₄[−] ions by the fungus, *Verticillium* sp. and surface trapping of the gold nanoparticles formed. *Angew. Chem. Int. Ed.* 40, 3585–3588.
- Nadagouda, M.N., Varma, R.S., 2008. Green synthesis of silver and palladium nanoparticles at room temperature using coffee and tea extract. *Green Chem.* 10, 859–862.
- Narayanan, K.B., Sakthivel, N., 2011. Green synthesis of biogenic metal nanoparticles by terrestrial and aquatic phototrophic and heterotrophic eukaryotes and biocompatible agents. *Adv. Colloid Interface Sci.* 169, 59–79.
- Nasrollahzadeh, M., Sajadi, S.M., Maham, M., 2015. Green synthesis of palladium nanoparticles using *Hippophae rhamnoides* Linn leaf extract and their catalytic activity for the Suzuki–Miyaura coupling in water. *J. Mol. Catal. A: Chem.* 396, 297–303.
- Parhi, P., Mohanty, C., Sahoo, S.K., 2012. Nanotechnology-based combinational drug delivery: an emerging approach for cancer therapy. *Drug Discovery Today* 17, 1044–1052.
- Petla, R.K., Vivekanandhan, S., Misra, M., Mohanty, A.K., Satyanarayana, N., 2012. Soybean (*Glycine max*) leaf extract based green synthesis of palladium nanoparticles. *J. Biomater. Nanobiotechnol.* 3, 14–19.
- Ramalingam, B., Parandhaman, T., Das, S.K., 2016. Antibacterial effects of biosynthesized silver nanoparticles on surface ultrastructure and nanomechanical properties of gram-negative bacteria viz. *Escherichia coli* and *Pseudomonas aeruginosa*. *ACS Appl. Mater. Interfaces* 8, 4963–4976.
- Sathishkumar, G., Gobinath, C., Karpagam, K., Hemamalini, V., Premkumar, K., Sivaramakrishnan, S., 2012. Phyto-synthesis of silver nanoscale particles using *Morinda citrifolia* L. and its inhibitory activity against human pathogens. *Colloids Surf. B: Biointerfaces* 95, 235–240.
- Sathishkumar, G., Bharti, R., Jha, P.K., Selvakumar, M., Dey, G., Jha, R., et al., 2015. Dietary flavone chrysin (5, 7-dihydroxyflavone ChR) functionalized highly-stable metal nanoformulations for improved anticancer applications. *RSC Adv.* 5, 89869–89878.
- Sathishkumar, G., Jha, P.K., Vignesh, V., Rajkuberan, C., Jeyaraj, M., Selvakumar, M., et al., 2016. Cannonball fruit (*Couroupita guianensis* Aubl.) extract mediated synthesis of gold nanoparticles and evaluation of its antioxidant activity. *J. Mol. Liq.* 215, 229–236.
- Shanthi, K., Sreevani, V., Vimala, K., Kannan, S., 2015. Cytotoxic effect of Palladium nanoparticles synthesized from *Syzygium aromaticum* aqueous extracts and induction of apoptosis in cervical carcinoma. *Proc. Nat. Acad. Sci. India Sect. B: Biol. Sci.* 1–12.
- Shen, X.S., Wang, G.Z., Hong, X., Zhu, W., 2009. Shape-controlled synthesis of palladium nanoparticles and their SPR/SERS properties. *Chin. J. Chem. Phys.* 22, 440–446.
- Shen, D.S., Philip, D., Mathew, J., 2012. Rapid green synthesis of Palladium nanoparticles using the dried leaf of *Anacardium occidentale*. *Spectrochim. Acta, Part A* 91, 35–38.
- Torre, L.A., Bray, F., Siegel, R.L., Ferlay, J., Lortet-Tieulent, J., Jemal, A., 2015. Global cancer statistics, 2012. *CA. Cancer J. Clin.* 65, 87–108.
- Vimala, R.T.V., Sathishkumar, G., Sivaramakrishnan, S., 2015. Optimization of reaction conditions to fabricate nano-silver using *Couroupita guianensis* Aubl. (leaf & fruit) and its enhanced larvicidal effect. *Spectrochim. Acta, Part A* 135, 110–115.
- Xie, J., Lee, J.Y., Wang, D.I., Ting, Y.P., 2007. Silver nanoplates: from biological to biomimetic synthesis. *ACS Nano* 1, 429–439.